DOI: 10.1002/ejic.201000578

Zinc(II) and Cadmium(II) Coordination Polymers Based on 3-(5*H*-Tetrazolyl)benzoate Ligand with Different Coordination Modes: Hydrothermal Syntheses, Crystal Structures and Ligand-Centered Luminescence

Feng Chen,[a,b] Mei-Feng Wu,[a,b] Guang-Ning Liu,[a,b] Ming-Sheng Wang,[a] Fa-Kun Zheng,*[a] Chen Yang,[a,b] Zhong-Ning Xu,[a,b] Zhi-Fa Liu,[a,b] Guo-Cong Guo,*[a] and Jin-Shun Huang[a]

Keywords: Cadmium / Zinc / Hydrothermal synthesis / Photochemistry / Luminescence

Hydrothermal reaction of Na(3-cba) (3-cba = 3-cyanobenzoate), NaN_3 and a metal salt with either 2,2′-bipyridine (2,2′-bipy) or 1,10-phenanthroline (phen) afforded four novel Zn^{II}/Cd^{II} polymers, which have been structurally characterized by single-crystal X-ray diffraction analysis. In situ [2 + 3] cycloaddition reaction of nitrile and azide in the presence of a Zn^{II} or Cd^{II} salt yielded the ligand 3-(5*H*-tetrazolyl)benzoate (3-tzba^{2-}) [3-H_2tzba = 3-(5*H*-tetrazolyl)benzoic acid]. The obtained polymers are formulated as $[Zn_2(3\text{-tzba})(N_3)(OH)(2,2'\text{-bipy})]$ (**1**), $[Zn(3\text{-tzba})(2,2'\text{-bipy})(H_2O)]\cdot 3H_2O$ (**2**), $[Zn_2(3\text{-tzba})_2(phen)_2]\cdot H_2O$ (**3**) and $[Cd_4(3\text{-tzba})_2(N_3)_4(2,2'\text{-bipy})_3]\cdot H_2O$ (**4**). A crystalline mixture of Zn^{II} polymers **1** and **2** with infinite ladder-like chain and zigzag chain structures, respectively, was obtained from the reaction in the presence of 2,2′-bipy. The replacement of 2,2′-bipy with phen as an auxiliary ligand yielded **3**, which shows a pearl-necklace-like chain structure. Further, the introduction of Cd^{II} instead of Zn^{II} resulted in the formation of **4**, which has a 2D corrugated layer structure. The 3-tzba^{2-} ligands display four different coordination modes in **1**–**4**, and modes μ_2-κN2:κO1,O2 (in **2**) and μ_3-κN3:κO1:κO2 (in **3**) are observed in tetrazolate-5-carboxylate polymers for the first time. Photoluminescent studies in the solid state at room and low temperature revealed that **1**–**4** exhibit interesting luminescent behaviors, and the relevant density of states (DOS) calculation results showed that their photoluminescence mainly originates from ligand-centered emission and is dependent on the organic ligand incorporated into the polymer.

Introduction

Exploration of metal-organic coordination polymers with novel molecular architectures and special applications such as catalysts, adsorption, sensors, molecular magnetism and optical materials, has been a focus of research for decades.[1] From the viewpoint of crystal engineering, the intrinsic geometric preferences of metal centers and the various coordination modes of bridging organic linkers are crucial factors in governing polymeric architectures.[2] Thus, rational selection of metal centers and organic ligands with suitable shape, functionality, flexibility, and symmetry plays a key role in synthesizing coordination polymers with desired structures and properties. Tetrazoles with similar pK_a values (ca. 4) to carboxylate acids and their substituted derivatives have been demonstrated as excellent organic linkers and have been employed extensively in building supramolecular assemblies with fascinating molecular architectures and\or promising applications.[3] Carboxylate-containing 5-substituted tetrazolate ligands, so-called tetrazolate-5-carboxylates, have attracted much attention because of their four nitrogen and two oxygen electron-donating atoms that allow them to serve as either multidentate ligands or as bridging building blocks in the construction of coordination polymers with novel topologies and properties.[4] However, the number of investigations of tetrazolate-5-carboxylate-containing polymers remains limited. Recently, we have used two bifunctional 1*H*-tetrazolate-5-carboxylate ligands, 1*H*-tetrazolate-5-acetic acid (H_2tza) and 1*H*-tetrazolate-5-formic acid (H_2tzf), in the synthesis of a series of coordination polymers/complexes, which possess interesting magnetic and luminescent properties.[5] Phenyl-ring-containing 3-(5*H*-tetrazolyl)benzoate (3-tzba^{2-}) and 4-(5*H*-tetrazolyl)-benzoate (4-tzba^{2-}) ligands have also been employed in the assembly of polymeric architectures in our laboratory. Two tzba-based (tzba = tetrazolylbenzoate; H_2tzba = tetrazolylbenzoic acid) coordination polymers, white-light-emitting [Zn(4-tzba)] and heterometallic [CdCo(3-tzba)(3-cba)(OH)-

[a] State Key Laboratory of Structural Chemistry, Fujian Institute of Research on the Structure of Matter, Chinese Academy of Sciences,
Fuzhou, Fujian 350002, P. R. China
Fax: +86-591-8371-4946
E-mail: zfk@fjirsm.ac.cn
[b] Graduate University, Chinese Academy of Sciences,
Beijing 100039, P. R. China
Supporting information for this article is available on the WWW under http://dx.doi.org/10.1002/ejic.201000578.

(H_2O)], were obtained with the aid of an in situ [2 + 3] cycloaddition reaction of cyanobenzoate (cba^-) with azide in the presence of Zn^{II}/Cd^{II} salts acting as Lewis acid catalysts.[6] In contrast with H_2tza and H_2tzf that are composed of acyclic spacers between the tetrazolate and carboxylate groups, the aromatic spacer containing H_2tzba ligands have increased conjugation in their systems, and their polymers should bear richer electronic behaviors such as magnetic and luminescent properties.[4e,7] As an extension to our research work, in this study we chose 3-$tzba^{2-}$ as an organic linker to create IIB metal-organic frameworks, while also incorporating 2,2′-bipyridine (2,2′-bipy) or 1,10-phenanthroline (phen) as auxiliary chelating ligands. Herein, we report the hydrothermal syntheses, crystal structures and photoluminescent properties of four new Zn^{II}/Cd^{II} coordination polymers, $[Zn_2(3\text{-tzba})(N_3)(OH)(2,2'\text{-bipy})]$ (**1**), $[Zn(3\text{-tzba})(2,2'\text{-bipy})(H_2O)]\cdot 3H_2O$ (**2**), $[Zn_2(3\text{-tzba})_2(phen)_2]\cdot H_2O$ (**3**) and $[Cd_4(3\text{-tzba})_2(N_3)_4(2,2'\text{-bipy})_3]\cdot H_2O$ (**4**). In **1**–**4**, the 3-$tzba^{2-}$ ligand adopts a diverse range of coordination modes (Scheme 1), of which modes II in **2** and III in **3** are observed in tetrazolate-5-carboxylate complexes for the first time. Polymers **1**–**4** display interesting photoluminescence in the solid state at room and cryogenic temperatures, and the photoluminescent mechanisms were investigated by means of density of states (DOS) calculations, which showed that the photoluminescence is mainly ascribed to ligand-centered emission and can be altered by introduction of different organic ligands into the polymer structure.

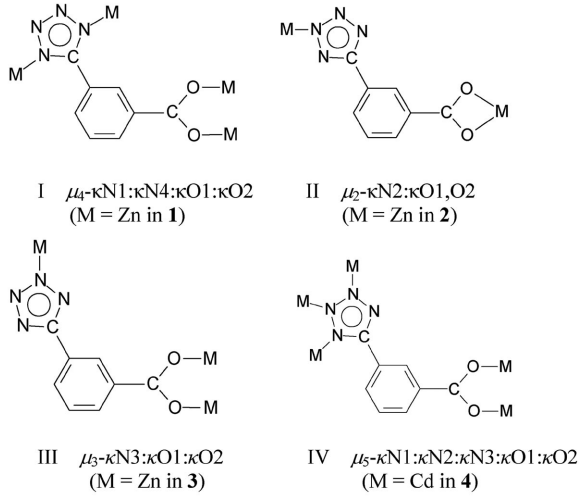

Scheme 1. Coordination modes of the 3-$tzba^{2-}$ ligand observed in this work.

Results and Discussion

Synthesis and IR Spectra

Due to the work of Sharpless et al. and advances in in situ synthetic technology, the preparation of 5-substituted 1*H*-tetrazoles can now be performed by a safe and convenient route.[8] In this study, we designed a hydrothermal synthetic route for **1**–**4** according to this synthetic technology, as shown in Scheme 2. The 3-$tzba^{2-}$ ligand in **1**–**4** was hydrothermally synthesized in situ by [2 + 3] cycloaddition reactions of Na(3-cba) and NaN_3 in the presence of Zn or Cd salts to act as Lewis acids. A mixture of colourless prism-shaped crystals of **1** and pale-yellow block-shaped crystals of **2** was obtained under these reaction conditions. The compounds were separated manually based on their distinct crystal shapes and colours. On the other hand, we attempted to vary the stoichiometric ratios of reactants and the reaction temperatures for the reaction mixture containing Na(3-cba), NaN_3, $Cd(NO_3)_2$ and phen, and only crystals of the 1D Cd^{II}–azido chain $[Cd(N_3)_2(phen)]$ were produced, without the 3-$tzba^{2-}$ ligand being involved.[9] The four 3-$tzba^{2-}$-based polymers **1**–**4** with 2,2′-bipy or phen as a coligand have 1D/2D molecular configurations. However, the hydrothermal reaction of a Zn^{II} salt and 3-H_2tzba in the absence of an auxiliary ligand produced a 3D polymer $[Zn(3\text{-tzba})]_n$.[10] This indicates that the secondary ligand, 2,2′-bipy or phen, exerts a synergic effect on the construction of 3-$tzba^{2-}$-based coordination polymers, and is not propitious for the formation of extended structures with high dimensionality. Meanwhile, it is noteworthy that the azide ion is concerned not only with the formation of the 3-$tzba^{2-}$ ligand, but also in coodinating with the metal atom in **1** and **4**. The synthetic strategy described herein may serve as a guide for the design and fabrication of coordination polymers with diverse structures. To the best of our knowledge, there are very few examples of tetrazolate-5-carboxylate coordination polymers into which a secondary chelating coligand has been introduced.[5a,7b] This is the first instance that auxiliary ligands, 2,2′-bipy or phen, have been introduced into $tzba^{2-}$-based coordination polymers with the aim of enriching their framework properties.

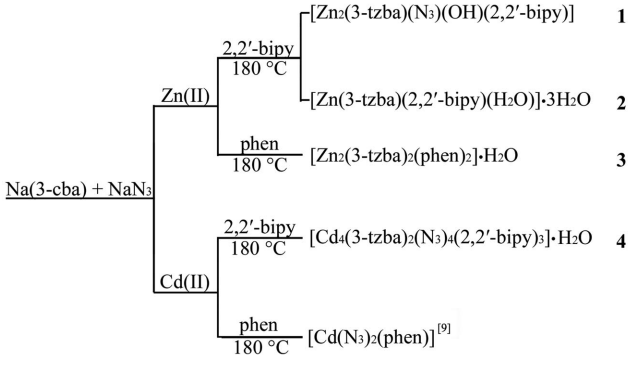

Scheme 2. Synthetic route for **1**–**4**.

Reliable IR peak assignments are made by comparing the IR spectra of **1**–**4** with that of the free 3-H_2tzba ligand, as displayed in Figure S1. For **1**–**4**, the characteristic stretching vibrations of tetrazolate, ν(tetrazolate), occur at 1617 and 1442 cm^{-1} for **1**, 1607 and 1443 cm^{-1} for **2**, 1604 and 1425 cm^{-1} for **3**, and 1595 and 1396 cm^{-1} for **4** in the IR spectra. Other important characteristic peaks in the IR spectra of **1**–**4** are the stretching vibrations of the carboxyl-

ate group, ν(COO). It is well known that the difference Δ between the asymmetrical and the symmetrical stretching frequencies of the carboxylate group, ν_{as}(COO) and ν_s(COO), respectively, are closely related to carboxylate coordination modes.[11] In the IR spectra the peaks at 1597 cm^{-1} for **1**, 1597 cm^{-1} for **2**, 1580 cm^{-1} for **3**, and 1581 cm^{-1} for **4** are attributed to ν_{as}(COO), whereas those at 1412 cm^{-1} for **1**, 1416 cm^{-1} for **2**, 1401 cm^{-1} for **3**, and 1386 cm^{-1} for **4** are ascribed to ν_s(COO). The Δ values of 185, 181, 179 and 195 cm^{-1} for **1**, **2**, **3** and **4**, respectively, are smaller than 200 cm^{-1}, which is indicative of a bidentate chelating or bridging coordination mode for the carboxylate groups. The characteristic peaks that are typical for the stretching vibration of the azide group, $\nu(N_3)$, should be clearly observable if this group is present in the compound.[12] The IR spectrum for polymer **1** with terminal azides exhibits a sharp and strong band at around 2079 cm^{-1}. The spectrum for azido-bridged **4** in the end-on (EO) mode shows a strong band around 2087 cm^{-1} with a shoulder peak at 2067 cm^{-1}.

Structure of 1

The structure of **1** features a 1D ladder-like chain formed by the linkage of the Zn^{II} centers by 3-tzba^{2-} ligands. The basic unit consists of two crystallographically independent Zn^{II} ions, one 3-tzba^{2-} anion, one 2,2′-bipy molecule, one terminal azide anion and one hydroxy group as demonstrated in Figure 1a. The Zn1 center is four-coordinate with a distorted tetrahedron geometry, whereas Zn2 is five-coordinate and can be represented by a slightly distorted trigonal-bipyramidal polyhedron. Ion Zn1 is bound to one carboxylate oxygen atom (O12) and one tetrazolate nitrogen atom (N14A) from two symmetry-related 3-tzba^{2-} ligands, one azide nitrogen atom (N3) and one hydroxy oxygen atom (O1) with the angles varying from 107.23(12) to 110.60(15)°, whereas for Zn2 the basal plane consists of one tetrazolate nitrogen atom (N11B), one hydroxy oxygen atom (O1) and one nitrogen atom (N21) from a 2,2′-bipy ligand, and the apical positions are occupied by one carboxylate oxygen atom (O11) and another 2,2′-bipy nitrogen atom (N22). The Zn2 ion is situated near the centre of the basal plane. The Zn–N/O bond lengths range from 1.907(3) to 2.144(2) Å and are well within the normal range. The tetrazolyl ring is seriously distorted with respect to the phenyl ring, displaying a large dihedral angle of 49.0(2)°. Notably, the azide ion in **1** takes part in not only in the formation of the 3-tzba^{2-} ligand, but is also coordinated to the metal ion, and displays a terminal coordination mode. Each 3-tzba^{2-} ligand acts as a tetradentate linker to ligate four Zn^{II} atoms in a μ_4-κN1:κN4:κO1:κO2 coordination mode I (Scheme 1), a mode which was also adopted by the ligands in previously reported tetrazolate-5-carboxylate coordination polymers.[4e]

There are dimeric [Zn(μ_2-COO)(μ_2-OH)Zn] units in **1** in which the Zn1 and Zn2 centers are doubly bridged by one carboxylate and one hydroxy group, with a Zn1···Zn2 distance of 3.295(2) Å and a Zn1–O1–Zn2 angle of 118.5(1)°. Each tzba^{2-} ligand bridges three dimeric units through a μ_2-1,4N tetrazolate group and carboxyl group to form a ladder-like chain extending along the *a*-axis (Figure 1b), which is an attractive structural characteristic of **1**. This kind of 1D ladder-like chain structure has been observed in many metal-organic frameworks,[13] but it is a rare occurance for tetrazolate polymers.[14]

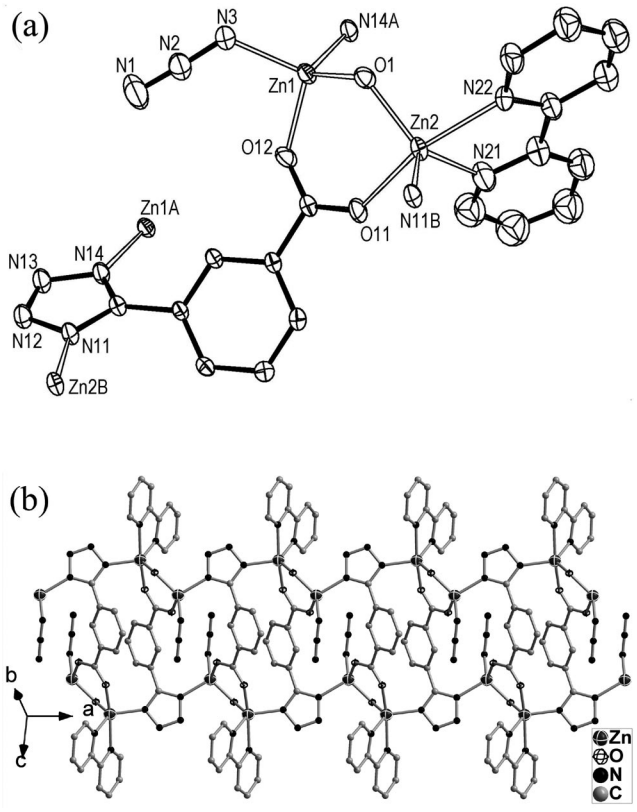

Figure 1. (a) ORTEP drawing of **1** with the thermal ellipsoids at the 30% probability level (symmetry codes: A: *–x*, 1 – *y*, 1 – *z*; B: 1 – *x*, 1 – *y*, 1 – *z*); (b) view of the 1D ladder-like chain of **1** along the *a*-axis. Hydrogen atoms are omitted for clarity.

Structure of 2

Polymer **2** has a 1D zigzag chain rather than the ladder-like chain structure observed in **1**. The asymmetric unit of **2** contains one [Zn(3-tzba)(2,2′-bipy)(H_2O)] motif as shown in Figure 2a and three lattice water molecules. The Zn1 center is surrounded by one 2,2′-bipy molecule, one coordinated water molecule and two symmetry-related 3-tzba^{2-} anions, and displays a distorted octahedral ZnN_3O_3 coordination environment. The Zn1–O_{3-tzba} bonds [2.175(2) and 2.224(2) Å] are slightly longer than the Zn1–$O1_{water}$ bond [2.094(2) Å]. This may be because the relatively small bite angle [O11–Zn1–O12 59.75(7)°] of the carboxylate group in the bidentate chelating mode weakens the Zn–O bonding interactions. The Zn–N distances [2.047(2)–2.159(2) Å] are in good agreement with those reported for six-coordinate Zn-tetrazolate complexes.[15] As depicted in Figure 2b, two

adjacent Zn centers are linked by a 3-tzba^{2-} ligand to afford a 1D zigzag chain. The Zn^{II} centers are spanned by a 3-tzba^{2-} ligand, with a distance of 11.027(11) Å between the metal ions. Each 3-tzba^{2-} ligand in **2** ligates two Zn centers exhibiting a novel μ_2-κN2:κO1,O2 coordination mode II (Scheme 1). Although numerous coordination modes for tetrazolate-5-carboxylate ligands have been found,[4–7] this is the first time that coordination mode II, as adopted by the 3-tzba^{2-} ligand in **2**, has been observed in a tetrazolate-5-carboxylate complex.

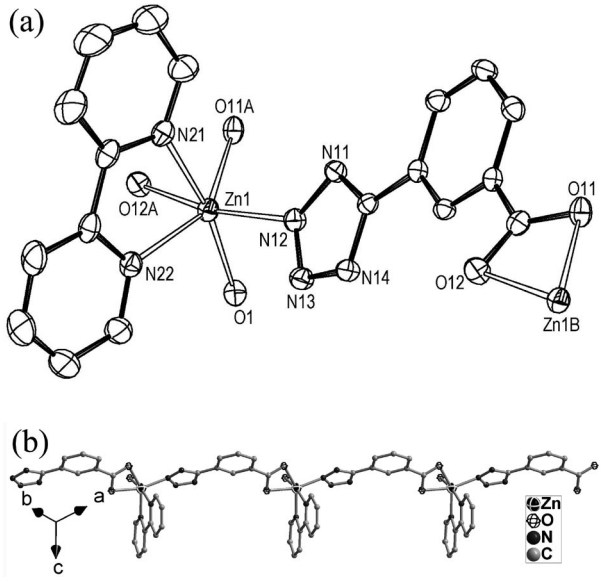

Figure 2. (a) ORTEP drawing of **2** with the thermal ellipsoids at the 30% probability level (symmetry codes: A: $x - 1$, $y + 1$, z; B: $x + 1$, $y - 1$, z); (b) 1D zigzag chain structure of **2**. Lattice water molecules and hydrogen atoms are omitted for clarity.

The neighbouring chains in **2** are connected by π–π stacking interactions between the tetrazolato and phenyl rings in an offset fashion to form a double chain structure with face-to-face distances of 3.442(2) and 3.498(2) Å, and dihedral angles of 4.72(2) and 4.29(3)°, respectively, as shown in Figure S2. The π–π stacking interactions impel the interchain Zn^{II} ions close to each other with the shortest Zn···Zn distance in the double chains being 5.094(1) Å. The lattice water molecules (O1W, O2W and O3W) construct 1D hydrogen-bonded water chains with an average O···O distance of 2.811(4) Å. The 1D water chain structures constitute potentially important forms of water.[16] Many fundamental biological processes appear to rely on the unique properties of water chains.[17] The nature of the structural constraints that stabilise 1D water chains has been explored.[18] The 1D water chains bridge the adjacent polymer double chains through O1···O1W [2.764(3) Å], O1W···N11 [2.938(3) Å] and O2W···N14 [2.902(4) Å] hydrogen bonds, to form a double layer structure parallel to the *ab* plane. Through the extension of the water chains along the *c*-axis double-layered nets are generated, and these in turn form a 3D supermolecular framework (Figure S2).

Structure of 3

Distinct from the structures of **1** and **2**, phen-containing **3** possesses a 1D pearl-necklace-like chain. The asymmetric unit in **3** contains two Zn^{II} centers, two 3-tzba^{2-} ligands, two phen molecules and one lattice water molecule (Figure 3a). The two crystallographically independent Zn^{II} atoms are both five-coordinate and are bound to one chelating phen molecule and three 3-tzba^{2-} ligands to furnish a distorted square-pyramidal [ZnN_3O_2] coordination sphere. This coordination sphere contains two nitrogen atoms from a chelating phen molecule, two carboxylate oxygen atoms from two different 3-tzba^{2-} ligands and one tetrazolate nitrogen atom. The Zn–O/N bond lengths range from 1.987(2) to 2.192(2) Å and are in accordance with values previously reported for five-coordinate Zn-tetrazole complexes.[3c] Interestingly, the carboxylate groups from the 3-tzba^{2-} ligands link two neighboring Zn ions to form a dimeric unit [Zn(μ_2-COO)$_2$Zn] that can be considered as a single pearl of the pearl-necklace-like chain structure, with the Zn1···Zn2 distance of 3.569(1) Å being different from the Zn···Zn distance in the dimeric unit in **1**. The dimeric units in **3** are doubly bridged by two 3-tzba^{2-} ligands to form an 18-membered ring. Finally, the dimeric units and the 18-membered rings are arranged in an alternating manner to form a 1D pearl-necklace-like chain along the *c*-axis (Figure 3b), with the distance between the Zn1 and Zn2 ions separated by the 3-tzba^{2-} ligand being 8.596(1) Å. The

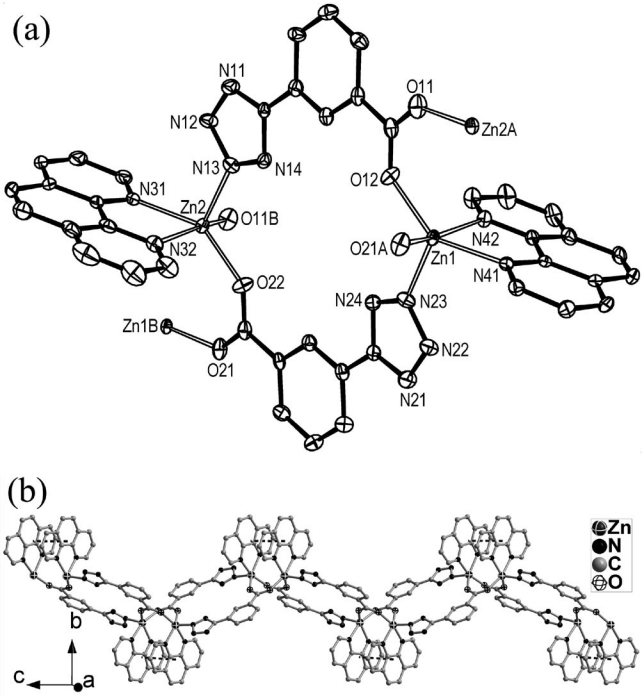

Figure 3. (a) ORTEP drawing of **3** with the thermal ellipsoids at the 30% probability level (symmetry codes: A: x, $0.5 - y$, $0.5 + z$; B: x, $0.5 - y$, $-0.5 + z$); (b) view of the 1D pearl-necklace-like chain structure of **3** that lies parallel to the *c*-axis. Black dotted lines indicate π–π stacking interactions between phen molecules in the intrachain dimeric unit. Lattice water molecules and hydrogen atoms are omitted for clarity.

3-tzba^{2-} ligand acts as a tridentate linker connecting three Zn^{II} centers in a μ_3-κN3:κO1:κO2 coordination mode III (Scheme 1), which is unprecedented in tetrazolate-5-carboxylate complexes.

The two chelating phen molecules in the intrachain dimeric unit are almost parallel with a dihedral angle of 4.23° and a face-to-face distance of 3.371(1) Å (Figure 3b), which denotes the existence of intrachain π–π stacking interactions. The lateral phen molecules adhering to the 1D chain protrude outwards and alternate on opposite sides of the chain. Moreover, phen molecules from adjacent chains are intercalated in a zipper-like mode, in a similar way to previously documented examples.[19] The interchain π–π stacking interactions [3.460(4) Å] extend the 1D chains into a 2D supramolecular sheet that lies parallel to the *bc* plane (Figure S3a). There are additional π–π stacking interactions between the tetrazolato and phenyl rings [3.211(2) and 3.399(2) Å], resulting in a 2D supramolecular network parallel to the *ac* plane (Figure S3b). Therefore, the 1D polymeric chains are stacked into a complicated 3D supramolecular architecture and are linked through bifurcated π–π stacking interactions.

Structure of 4

Polymer **4** presents an interesting 2D layer structure built from the fusion of Cd^{II}–azido inorganic chains and 3-tzba^{2-} ligands. The asymmetric unit consists of four Cd^{II} ions, two 3-tzba^{2-} ligands, four bridging azide ions, three chelating 2,2′-bipy molecules and two lattice water molecules (Figure 4a). The four crystallographically independent Cd centers are all six-coordinate and have distorted octahedral geometries. Nevertheless, their coordination spheres are different. The Cd1 ion is surrounded by four nitrogen atoms from two 3-tzba^{2-} ligands and two azide groups, and two oxygen atoms from another two 3-tzba^{2-} ligands. The Cd2 center is bound to six nitrogen atoms from one 2,2′-bipy molecule, two 3-tzba^{2-} ligands, and two azide groups. The Cd3 and Cd4 centers are coordinated by five nitrogen atoms from one 2,2′-bipy molecule, one 3-tzba^{2-} ligand, and two azide groups, and one oxygen atom from another 3-tzba^{2-} ligand. All of the Cd–O/N distances range from 2.242(3) to 2.466(3) Å, which are comparable with those previously reported for six-coordinate cadmium complexes.[3c,20] The 1D Cd^{II}–azido chains are further connected by 3-tzba^{2-} ligands to afford a 2D corrugated layer network parallel to the *ac* plane. In the two crystallographically independent 3-tzba^{2-} ligands, the dihedral angles between the tetrazolato rings and corresponding aromatic rings are 18.7(5)° and 24.4(5)°. In order to shed light on the structure of **4** we have omitted the auxiliary chelating 2,2′-bipy ligands from the structural diagram, as depicted in Figure 4b. As shown in Figure 4b the adjacent Cd^{II} atoms are connected by single azido bridges in the EO mode to produce 1D Cd^{II}–azido inorganic chains that lie along the *c*-axis. The intrachain Cd···Cd distances are 3.702(1) Å (Cd1B···Cd3), 3.953(1) Å (Cd3···Cd2), 4.003(1) Å (Cd2···Cd4) and 3.756(1) Å (Cd4···Cd1). In contrast to **1**–**3**, the bridging 3-tzba^{2-} ligand in **4** adopts the unusual coordination mode IV (Scheme 1), μ_5-κN1:κN2:κN3:κO1:κO2, which links five Cd^{II} centers. Tetrazolate-5-carboxylate ligands displaying such a coordination mode have occasionally been used in the construction of metal-organic frameworks.[21]

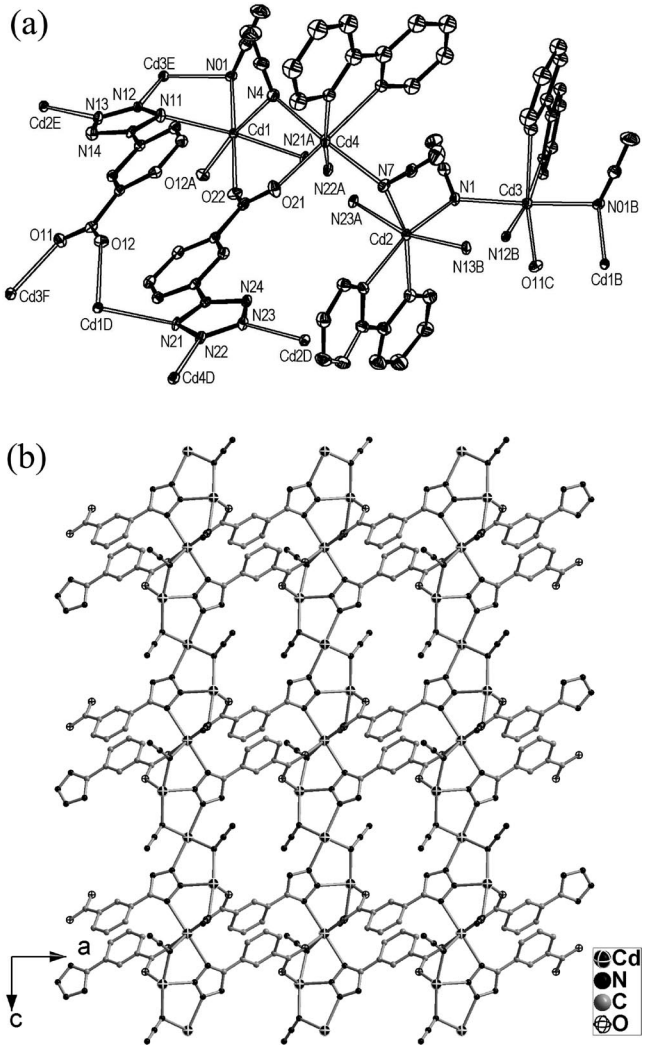

Figure 4. (a) ORTEP drawing of **4** with the thermal ellipsoids at the 30% probability level (symmetry codes: A: 0.5 + *x*, 0.5 – *y*, *z*; B: *x*, *y*, 1 + *z*; C: 0.5 + *x*, 0.5 – *y*, 1 + *z*; D: –0.5 + *x*, 0.5 – *y*, *z*; E: *x*, *y*, –1 + *z*; F: –0.5 + *x*, 0.5 – *y*, –1 + *z*); (b) view of the 2D sheet network of **4** that lies parallel to the *ac* plane. Chelating 2,2′-bipy ligands and lattice water molecules are omitted for clarity.

The utilization of metal clusters or inorganic chains as secondary building units in place of naked metal ions has provided a promising pathway for the generation of novel coordination polymers.[22] In this work, three distinct metal moieties exist: [Zn(μ_2-COO)(μ_2-OH)Zn] dimeric unit in **1**, [Zn(μ_2-COO)$_2$Zn] dimeric unit in **3**, and Cd^{II}–azido inorganic chains in **4**. These different metal units result in the formation of various metal-directed polymers, and greatly enrich the architectures adopted by these polymers. In **1**–**4**,

the bridging 3-tzba^{2-} ligand displays flexible coordination styles (Scheme 1): μ_4-κN1:κN4:κO1:κO2 in **1**, μ_2-κN2:κO1,O2 in **2**, μ_3-κN3:κO1:κO2 in **3**, and μ_5-κN1:κN2:κN3:κO1:κO2 in **4**. This is the first time that coordination modes II (in **2**) and III (in **3**) have been observed in tetrazolate-5-carboxylate complexes. The different coordination modes of the 3-tzba^{2-} linker offers the possibility of the formation of coordination polymers with different structures. However, the ionic radii of the metal centers also influence the stucture of the polymeric frameworks. The Cd^{II} ion has a larger ionic radius than Zn^{II}, which leads to these ions having different coordination numbers and ligating tendencies upon complexation. Compared to the six-coordinate Cd^{II} ions in **4**, the Zn^{II} ions in **1**–**3** prefer to display lower coordination numbers: four/five-, six-, and five-coordinate Zn^{II} centers in **1**, **2**, and **3**, respectively. Of particular interest is the Cd1 ion in **4** that is bound to four bulky 3-tzba^{2-} ligands. As a result, the Zn^{II} polymers **1**–**3** feature 1D chains that have a lower dimensionality relative to the 2D Cd^{II} polymer **4**. Finally, the introduction of auxiliary rigid 2,2′-bipy or phen chelating ligands to the frameworks adds further variation to the molecular architectures formed, which is maybe due to the intrinsic basicity of the ligands and steric effects. Based on the forementioned facts, the 3-tzba^{2-} ligand, metal centers and secondary ligands have a cooperative impact on the self-assembly of coordination polymers.

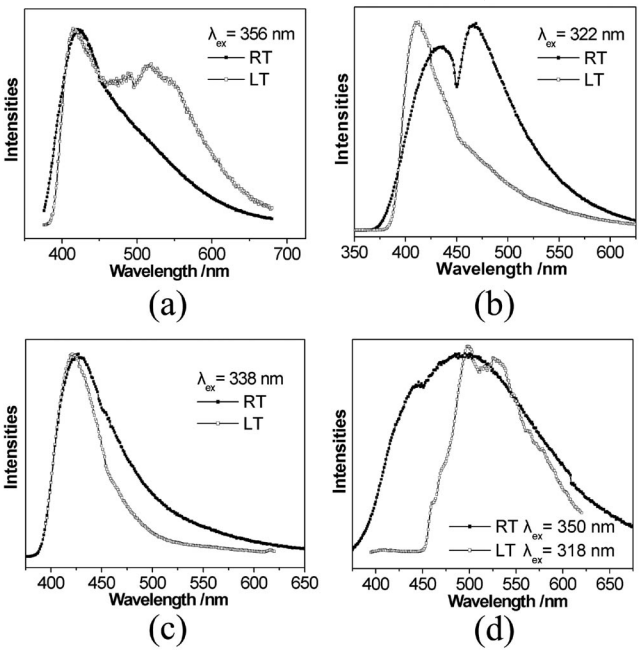

Figure 5. Solid-state emission spectra for **1** (a), **2** (b), **3** (c) and **4** (d) recorded at room temperature (RT) and –150 °C (LT).

Luminescent Properties

It is well known that d^{10} transition metal complexes exhibit interesting luminescent emission bands, which originate from different luminescent sources such as metal-to-ligand, ligand-to-metal, metal-centered and ligand-centered charge transfer processes.[23] Luminescent Zn^{II} and Cd^{II} coordination complexes containing aromatic ligands occupy a special position as they have potential application as visible light emitters in a number of technologically advanced fields.[24] For example, some Zn^{II} complexes have been reported to be useful organic light-emitting diodes (OLEDs).[25]

The reflectance diffusion spectra of **1**–**4** and the 3-H_2tzba ligand are shown in Figure S4, and indicate that **1**–**4** display intense transitions in the high energy region (300–395 nm) and almost no absorption in the visible region (400–800 nm) except in the case of **3**, which is a brownish solid. The absorption bands in the UV range can be assigned to ligand-based π–π* charge transfer. The solid-state excitation and emission spectra for **1**–**4** recorded at ambient and cryogenic temperatures, together with the Commission Internationale de l'Eclairage (CIE) chromaticity coordinates, are shown in Figures S5, 5 and S6, respectively. For comparison with the emission spectra of the coordination polymers, the emission spectra of the 2,2′-bipy, phen and 3-H_2tzba ligands, recorded at room temperature, are illustrated in Figure S7.

When excited by 356, 322 and 338 nm light at ambient temperature, polymers **1**–**3** display blue luminescent emission bands at 420 nm for **1**, 437 and 465 nm for **2**, and 427 nm for **3**. Upon excitation at 350 nm under the same conditions, **4** exhibits a blue emission maximum at about 495 nm. The CIE chromaticity coordinates are (0.21, 0.23) for **1**, (0.18, 0.20) for **2**, (0.19, 0.15) for **3** and (0.27, 0.35) for **4** (Figure S6). The lifetime of the maximum emissions peaks were measured as 3.19 ns for **1**, 8.20 ns (for the 437 nm peak) and 5.35 ns (for the 465 nm peak) for **2**, 6.11 ns for **3** and 3.92 ns for **4**, which suggests that these emissions should be assigned to room-temperature fluorescence.

In Zn^{II}/Cd^{II} coordination complexes two types of electronic exticted state transition, ligand-to-ligand charge transfer (LLCT) and ligand-to-metal charge transfer (LMCT), are common.[26] To understand better the room-temperature photoluminescent mechanisms, the optimized structures for polymers **1**–**3** were theoretically calculated by evaluation of the density of states (DOS) for these complexes. These calculations were performed with the CASTEP code based on density functional theory with a plane-wave expansion of the wave functions, instead of the time-dependent density functional theory (TDDFT) that is suitable for isolated structures.[27] The total and partial DOS for **1**–**3** are illustrated in Figure 6. The Zn^{II} ions make little or no contribution to the top of the valence bands (VBs) or to the bottom of the conduction bands (CBs). For **1**, on the basis of the calculation results, the VBs between energy –5.0 eV and the Fermi level (0.0 eV) mainly originate from the p-π orbitals of the 3-tzba^{2-}, 2,2′-bipy and azide ligands, whereas the p-π* antibonding orbitals of the 3-tzba^{2-} and 2,2′-bipy ligands contribute mainly to the CBs

with energy values between 1.5 and 4.5 eV (Figure 6a). Accordingly, it can be considered that the emission band in the spectrum of **1** originates from a mixed ligand-ligand charge transition. Furthermore, based on the comparison of the location and profile of the maximum emission peak in the spectrum of **1** with those in the spectra of the free ligands 3-H_2tzba (407 nm) and 2,2′-bipy (543 nm), the emission band centered at 420 nm in the spectrum of **1** is ascribed to a 3-tzba^{2-} ligand-centered charge transition, in agreement with previous reported data for analogous 5-substituted tetrazolate complexes.[5a,28]

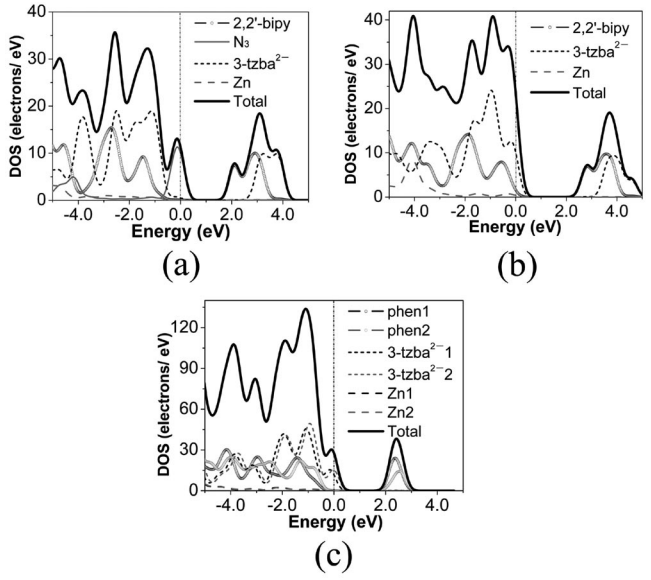

Figure 6. Total and partial DOS for **1** (a), **2** (b) and **3** (c). The position of the Fermi level is set at 0.0 eV.

According to the theoretical results for **2** and **3** (Figures 6b and c), the origin of the spectral emissions observed in their spectra can be attributed to ligand-centered charge transitions based on the 2,2′-bipy and 3-tzba^{2-} ligands for **2**, and the phen and 3-tzba^{2-} ligands for **3**. Notably, in the emission spectrum of **2** twin peaks (at 437 and 465 nm) appear, which may be caused by the mixed-ligand system and supramolecular interactions such as hydrogen bonds and π–π stacking interactions, resulting in multiple electronic transitions with close transition energies. In contrast to the free phen ligand that emitted at 404 nm, **3** shows a fluorescent redshifted emission maximum at 427 nm, which indicates that the luminescence of **3** is due to phen-centered charge transfer.

Theoretical calculations by the DOS method cannot be carried out for **4** owing to its complicated molecular structure. Ligand-centered charge transfer should be responsible for the broad band ranging from 400 to 600 nm in the emission spectrum of **4**. This phenomenon has also been observed in zinc(II) and cadmium(II) coordination polymers containing heterocyclic ligands.[26,29] It is noteworthy that the emission band of **4** exhibits an obvious redshift in contrast to those of **1**–**3**; this is partly due to the metal ions. Compared with the Zn^{II} ion, the Cd^{II} ion has less of an electron-pulling effect on the organic ligands, which is concomitant with the smaller HOMO–LUMO gaps of these complexes with respect to the Zn^{II} complexes.

Now we turn our attention to the photoluminescent phenomena at low temperature when the CIE chromaticity coordinates for the complexes are (0.26, 0.32) for **1**, (0.18, 0.14) for **2**, (0.17, 0.09) for **3** and (0.28, 0.52) for **4** (Figure S6). When frozen at –150 °C, **1** exhibits an unusual green emission at 528 nm in addition to the characteristic blue emission at 420 nm. The solid-state lifetimes of 3.68 ns for the 420 nm peak and 14.40 μs for the 528 nm peak reveal that the emission at 528 nm is phosphorescence, which is quenched at room temperature. It is well known that the singlet (^{1}A) and triplet (^{3}A) excited states are thermally coupled. As the temperature increases, the electrons located in the ^{3}A state are promoted to the ^{1}A state by phonon absorption, which results in phosphorescent quenching at low temperature.[30] The spectrum of polymer **2** recorded at low temperature displays only a blueshifted maximum emission at 412 nm (τ = 16.09 ns), which is comparable to the emission at 437 nm in the spectrum recorded at room temperature. Notably, the emission peak at 465 nm in the room-temperature spectrum almost vanishes in the low-temperature spectrum. This can be ascribed to the restriction at low temperatures of the electronic multiphonon nonradiative relaxation from a high-energy to the lowest-energy excited state.[31] However, the low-temperature spectrum of **3** shows a similar emission centered at 420 nm (τ = 7.14 ns) that is also seen in the room-temperature spectrum. The low-temperature emission peak in the spectrum of **4** is narrow and asymmetric, and has a redshifted maximum at 532 nm (τ = 4.24 ns) upon excitation with 318 nm light, which is blueshifted with respect to the 350 nm excitation light employed to recorded the room-temperature spectrum. The 532 nm peak shows a long low-energy tail that suggests the presence of an unresolved vibronic structure with the complex.[32]

As mentioned above, the nature of organic ligands undoubtedly plays a critical role in the luminescent emissions of **1**–**4**. Variation in temperature also has a profound effect on the luminescent properties. The excitation wavelengths for **1**–**4** fall in the range of commercially available luminescent devices, and **1**–**4** show broad visible emission bands and are insoluble in most solvents such as ethanol, chloroform, acetone, acetonitrile, benzene and water. Therefore, **1**–**4** could be promising luminescent materials for solid-state lighting applications. Although the synthesis of luminescent materials is still a challenge, incorporating conjugated organic ligands into coordination polymers is an efficient method for preparing materials with desired luminescent properties.

Conclusions

We have succeeded in synthesizing four new Zn^{II}/Cd^{II} coordination polymers based on the 3-tzba^{2-} ligand using hydrothermal synthesis methods. The incorporation of chelating auxiliary ligands into the complexes (2,2′-bipy and

phen) leads to 1D chains (**1**, **2** and **3**) and 2D layer nets (**4**). Structural analyses reveal the occurrence of three different metal moieties: [Zn(μ_2-COO)(μ_2-OH)Zn] dimeric unit in **1**, [Zn(μ_2-COO)$_2$Zn] dimeric unit in **3** and Cd^{II}–azido inorganic chains in **4**. This work indicates that the 3-tzba^{2-} ligand, metal ions and auxiliary ligands have a cooperative impact on the final molecular architectures of the polymer complexes. In **1**–**4**, four distinct coordination modes of the 3-tzba^{2-} ligand are observed, and two unprecedented coordination modes of the tetrazolate-5-carboxylate ligand are found: μ_2-κN2:κO1,O2 in **2** and μ_3-κN3:κO1:κO2 in **3**. These Zn^{II}/Cd^{II} coordination polymers, which contain auxiliary ligands, display ligand-centered luminescent emissions. Temperature exerts an influence on the luminescent emissions. Further endeavors involving the exploration of 3-tzba^{2-}-based coordination polymers as promising luminescent materials are underway in our research group.

Experimental Section

General: The sodium salt of 3-Hcba (3-Hcba = 3-cyanobenzoic acid), Na(3-cba), was prepared by the reaction of 3-Hcba and NaOH in an equivalent molar ratio in hot distilled water. All chemicals except for Na(3-cba) were purchased commercially and used without further purification. **Caution!** Sodium azide and tetrazolate compounds are energetic materials that might explode under certain conditions. Only a small amount of material should be prepared at any one time and must be handled with care. Elemental microanalyses of C, H and N were determined with a Vario EL III elemental analyzer. The FT-IR spectra were recorded in the 4000–400 cm^{-1} range with a Perkin–Elmer Spectrum One Spectrometer using KBr pellets. Powder X-ray diffraction data were collected with a MiniFlexII powder diffractometer for **2** and **3**, and an X'Pert Pro powder diffractometer for **4**, both diffractometers were equipped with a Cu-K_α radiation source (λ = 1.54056 Å). A step size of 0.05° and counting time of 5°/min were applied over a 2θ range of 5.00–65.00°. Optical diffuse reflectance spectra were measured at room temperature with a computer-controlled PE Lambda 900 UV/Vis spectrophotometer. The sample was ground to fine powder and pressed onto a thin glass-slide holder with a $BaSO_4$ base. Photoluminescence (PL) and lifetime values were measured with an Edinburgh Instruments Analyzer model FLS920 equipped with a 450 W steady-state xenon lamp (ozone-free) with the samples prepared as pressed KBr pellets. A 399 nm high-pass filter was applied when performing PL determinations.

Calculation of the Density of States (DOS): The X-ray crystallographic data for **1**–**3** were used to calculate the density of states (DOS) for these complexes. The calculation of the DOS was carried out with density functional theory (DFT) with one of the three nonlocal gradient corrected exchange-correlation functionals (GGA-PBE), and performed with the CASTEP code in the Materials Studio v4.0 software package,[33,34] which uses a plane wave basis set for the valence electrons and norm-conserving pseudopotential[35] for the core electrons. The number of plane waves included in the basis was determined by a cutoff energy of 300.0 eV, and the numerical integration of the Brillouin zone was performed with a 1 × 1 × 1 Monkhorst–Pack k-point sampling for the accurate calculation of the optical properties of the complexes. Other parameters in the calculations were set to the CASTEP code default values.

Synthetic Procedures

[Zn_2(3-tzba)(N_3)(OH)(2,2′-bipy)] (1) and [Zn(3-tzba)(2,2′-bipy)(H_2O)]·3H_2O (2): A mixture of $ZnBr_2$ (0.225 g, 1.00 mmol), NaN_3 (0.065 g, 1.00 mmol), Na(3-cba) (0.085 g, 0.50 mmol), 2,2′-bipy (0.078 g, 0.50 mmol) and H_2O (8 mL) was placed in a Teflon-lined stainless steel container. The mixture was heated at 180 °C for 3 d, and then cooled to room temperature and allowed to stand for 3 d. Colourless prism-shaped crystals of **1** and pale-yellow block-shaped crystals of **2** suitable for XRD were obtained simultaneously. The mixture of crystals was washed with distilled water, dried in air, and then separated manually. Yield: 29 mg (11% based on Zn) for **1**. $C_{18}H_{13}N_9O_3Zn_2$ (534.11): calcd. C 40.47, H 2.44, N 23.61; found C 40.38, H 2.40, N 23.72. IR (KBr): $\tilde{\nu}$ = 3391 (br.), 3368 (w), 2079 (s), 1617 (s), 1597 (s), 1572 (s), 1516 (m), 1474 (m), 1442 (s), 1412 (s), 1378 (s), 1316 (m), 1248 (w), 1157 (w), 1023 (s), 933 (w), 765 (s), 753 (s), 734 (s), 690 (m), 653 (m), 606 (w), 548 (s), 470 (m), 415 (m) cm^{-1}. Yield: 268 mg (56% based on Zn) for **2**. $C_{18}H_{20}N_6O_6Zn$ (481.79): calcd. C 44.87, H 4.15, N 17.43; found C 45.22, H 4.03, N 17.24. IR (KBr): $\tilde{\nu}$ = 3231 (br), 1607 (m), 1597 (m), 1577 (m), 1549 (s), 1506 (m), 1474 (m), 1443 (s), 1416 (s), 1315 (m), 1247 (w), 1220 (w), 1159 (m), 1024 (w), 893 (w), 763 (s), 735 (s), 653 (m), 410 (m) cm^{-1}.

[Zn_2(3-tzba)$_2$(phen)$_2$]·H_2O (3): A mixture of $ZnBr_2$ (0.225 g, 1.00 mmol), NaN_3 (0.065 g, 1.00 mmol), Na(3-cba) (0.085 g, 0.50 mmol), phen (0.099 g, 0.50 mmol) and H_2O (8 mL) was placed in a Teflon-lined stainless steel container. The mixture was heated at 180 °C for 3 d, then cooled to room temperature and allowed to stand for 2 d. Brown prism-shaped crystals suitable for X-ray analysis were obtained, washed with distilled water, and dried in air. Yield: 141 mg (32% based on Zn). $C_{40}H_{26}N_{12}O_5Zn_2$ (885.47): calcd. C 54.25, H 2.93, N 18.99; found C 54.50, H 2.86, N 19.20. IR (KBr): $\tilde{\nu}$ = 3463 (br.), 3080 (w), 1629 (s), 1604 (s), 1580 (s), 1517 (m), 1464 (w), 1425 (s), 1401 (s), 1368 (m), 1226 (w), 1170 (w), 1103 (m), 1076 (w), 847 (m), 786 (w), 725 (s), 686 (w), 663 (w), 486 (w), 422 (w) cm^{-1}.

[Cd_4(3-tzba)$_2$(N_3)$_4$(2,2′-bipy)$_3$]·H_2O (4): A mixture of $Cd(NO_3)_2$·4H_2O (0.308 g, 1.00 mmol), NaN_3 (0.065 g, 1.00 mmol), Na(3-cba) (0.085 g, 0.50 mmol), 2,2′-bipy (0.078 g, 0.50 mmol) and H_2O (8 mL) was placed in a Teflon-lined stainless steel container. The mixture was heated at 180 °C for 2 d, then cooled to room temperature and allowed to stand for 2 d. Pale-yellow prism-shaped crystals suitable for X-ray analysis were obtained, washed with distilled water, and dried in air. Yield: 97 mg (26% based on Cd). $C_{46}H_{34}Cd_4N_{26}O_5$ (1480.59): calcd. C 37.31, H 2.30, N 24.60; found C 37.45, H 2.28, N 23.69. IR (KBr): $\tilde{\nu}$ = 3436 (br.), 2087 (s), 2067 (s), 1595 (m), 1581 (s), 1556 (s), 1507 (w), 1474 (w), 1440 (m), 1396 (s), 1386 (s), 1345 (w), 1291 (w), 1157 (w), 1017 (w), 747 (m), 651 (w) cm^{-1}.

Single-Crystal Structure Determinations: Single crystals of **1**–**4** were mounted on glass fibers. Data collections were performed with a Rigaku Saturn-724 CCD diffractometer for **1** and **2**, a Rigaku Saturn-70 CCD diffractometer for **3**, and a Rigaku SCX-mini CCD diffractometer for **4**. All diffractometers were equipped with graphite-monochromated Mo-K_α radiation sources (λ = 0.71073 Å), and collections were performed in the ω-scan mode. The structures were solved by direct methods with the SHELXTL (version 5) crystallographic software package.[36] The structures were refined by full-matrix least-squares refinement on F^2. Metal atoms were located from the electron-density maps and were refined anisotropically, all other non-hydrogen atoms were located from the difference Fourier maps and were refined anisotropically. The hydrogen atoms of the coordinated water molecules were located from the difference Fou-

Table 1. Crystal data and structure refinements for **1**–**4**.

Polymer	**1**	**2**	**3**	**4**
Empirical formula	$C_{18}H_{13}N_9O_3Zn_2$	$C_{18}H_{20}N_6O_6Zn$	$C_{40}H_{26}N_{12}O_5Zn_2$	$C_{46}H_{34}Cd_4N_{26}O_5$
Formula mass	534.11	481.79	885.47	1480.59
Crystal system	triclinic	triclinic	monoclinic	orthorhombic
Space group	$P\bar{1}$	$P\bar{1}$	$P2_1/c$	$Pna2_1$
a [Å]	8.140(4)	9.1494(19)	8.7598(19)	17.680(3)
b [Å]	10.129(5)	10.667(2)	20.608(4)	24.516(4)
c [Å]	12.671(7)	12.596(3)	20.080(4)	12.4655(18)
α [°]	103.219(6)	68.585(8)	90	90
β [°]	91.981(5)	75.534(10)	98.586(4)	90
γ [°]	98.218(8)	67.117(9)	90	90
V [Å^3]	1004.2(9)	1046.0(4)	3584.3(13)	5403.2(14)
Z	2	2	4	4
T [K]	293(2)	293(2)	293(2)	293(2)
D_c [g/cm^3]	1.767	1.530	1.641	1.820
μ [mm^{-1}]	2.432	1.222	1.405	1.624
F(000)	536	496	1800	2896
2θ range [°]	2.53–27.46	2.82–25.00	2.55–25.50	2.75–25.00
Unique reflections (R_{int})	4536 (0.0384)	3645 (0.0260)	6512 (0.0422)	9456 (0.0309)
GOF (F^2)	1.030	1.083	1.067	1.036
Final R indices [$I > 2\sigma(I)$][a]	R_1 = 0.0581 wR_2 = 0.1668	R_1 = 0.0409 wR_2 = 0.1107	R_1 = 0.0579 wR_2 = 0.1353	R_1 = 0.0359 wR_2 = 0.0842
Final R indices (all data)[a]	R_1 = 0.0794 wR_2 = 0.1855	R_1 = 0.0460 wR_2 = 0.1131	R_1 = 0.0658 wR_2 = 0.1403	R_1 = 0.0370 wR_2 = 0.0852
Max./min. residual electron density [e Å^{-3}]	1.540/–1.264	1.547/–0.451	0.982/–0.536	1.675/–0.944
CCDC-	771924	771925	771926	771927

[a] $R_1 = \Sigma(F_o - F_c)/\Sigma F_o$; $wR_2 = [\Sigma w(F_o^2 - F_c^2)^2/\Sigma w(F_o^2)^2]^{1/2}$.

rier maps, and the O–H distances (0.85 Å) and U_{iso}(H) [U_{iso}(H) = 1.2U_{eq}(O)] values were restrained. Hydrogen atoms of the lattice water molecules are not included in the structural models for **2** and **4**. Other hydrogen atoms were added according to theoretical models. ISOR and PART instructions were applied to the 2,2′-bipyridine rings of **1** and **4** to model the atomic disorder. Pertinent crystal data and structure refinement results for **1**–**4** are summarized in Table 1, and selected bonds lengths and angles for these complexes are provided in Tables S1–S4. CCDC-771924 (**1**), -771925 (**2**), -771926 (**3**) and -771927 (**4**) contain the supplementary crystallographic data for this paper. These data are available free of charge from The Cambridge Crystallographic Data Centre via www.ccdc.cam.ac.uk/data_request/cif.

Supporting Information (see footnote on the first page of this article): Selected bond lengths [Å] and angles [°] for **1**–**4**. IR spectra of **1**–**4** and 3-H_2tzba, supramolecular structures of **2** and **3**, excitation spectra and reflectance diffusion spectra of **1**–**4**, emission spectra of the organic ligands, CIE chromaticity diagram for **1**–**4**, and powder diffraction patterns for **2**–**4**.

Acknowledgments

We gratefully acknowledge financial support from the 973 Program (2006CB932900 and 2007CB936703), the National Nature Science Foundation of China (20871115) and the Fujian Province (A0420002).

[1] a) P. J. Hagrman, D. Hagrman, J. Zubieta, *Angew. Chem. Int. Ed.* **1999**, *38*, 2639–2684; b) O. M. Yaghi, M. O'Keeffe, N. W. Ockwig, H. K. Chae, M. Eddaoudi, J. Kim, *Nature* **2003**, *423*, 705–714; c) A. B. Gaspar, V. Ksenofontov, M. Seredyuk, P. Gütlich, *Coord. Chem. Rev.* **2005**, *249*, 2661–2676; d) S. Kitagawa, R. Matsuda, *Coord. Chem. Rev.* **2007**, *251*, 2490–2509; e) A. A. Martí, S. Jockusch, N. Stevens, J. Y. Ju, N. J. Turro, *Acc. Chem. Res.* **2007**, *40*, 402–409; f) B. V. Harbuzaru, A. Corma, F. Rey, P. Atienzar, J. L. Jordá, H. García, D. Ananias, L. D. Carlos, J. Rocha, *Angew. Chem. Int. Ed.* **2008**, *47*, 1080–1083; g) J. Y. Lee, O. K. Farha, J. Roberts, K. A. Scheidt, S. T. Nguyen, J. T. Hupp, *Chem. Soc. Rev.* **2009**, *38*, 1450–1459.

[2] a) S. Kitagawa, S. Noro, T. Nakamura, *Chem. Commun.* **2006**, 701–707; b) T. M. Klapötke, C. M. Sabaté, *Chem. Mater.* **2008**, *20*, 3629–3637; c) A. Białońska, R. Bronisz, M. Weselski, *Inorg. Chem.* **2008**, *47*, 4436–4438.

[3] a) T. T. Luo, H. L. Tsai, S. L. Yang, Y. H. Liu, R. D. Yadav, C. C. Su, C. H. Ueng, L. G. Lin, K. L. Lu, *Angew. Chem. Int. Ed.* **2005**, *44*, 6063–6067; b) M. Dincă, J. R. Long, *J. Am. Chem. Soc.* **2007**, *129*, 11172–11176; c) H. Zhao, Z. R. Qu, H. Y. Ye, R. G. Xiong, *Chem. Soc. Rev.* **2008**, *37*, 84–100.

[4] a) F. Nouar, J. F. Eubank, T. Bousquet, L. Wojtas, M. J. Zaworotko, M. Eddaoudi, *J. Am. Chem. Soc.* **2008**, *130*, 1833–1835; b) Q. X. Jia, Y. Q. Wang, Q. Yue, Q. L. Wang, E. Q. Gao, *Chem. Commun.* **2008**, 4894–4896; c) W. B. Yang, X. Lin, A. J. Blake, C. Wilson, P. Hubberstey, N. R. Champness, M. Schröder, *CrystEngComm* **2009**, *11*, 67–81; d) V. Hartdegen, T. M. Klapötke, S. M. Sproll, *Inorg. Chem.* **2009**, *48*, 9549–9556; e) W. C. Song, J. R. Li, P. C. Song, Y. Tao, Q. Yu, X. L. Tong, X. H. Bu, *Inorg. Chem.* **2009**, *48*, 3792–3799.

[5] a) M. F. Wu, F. K. Zheng, A. Q. Wu, Y. Li, M. S. Wang, W. W. Zhou, F. Chen, G. C. Guo, J. S. Huang, *CrystEngComm* **2010**, *12*, 260–269; b) A. Q. Wu, Q. Y. Chen, M. F. Wu, F. K. Zheng, F. Chen, G. C. Guo, J. S. Huang, *Aust. J. Chem.* **2009**, *62*, 1622–1630; c) Q. Y. Chen, Y. Li, F. K. Zheng, W. Q. Zou, M. F. Wu, G. C. Guo, A. Q. Wu, J. S. Huang, *Inorg. Chem. Commun.* **2008**, *11*, 969–971; d) M. F. Wu, F. K. Zheng, G. Xu, A. Q. Wu, Y. Li, H. F. Chen, S. P. Guo, F. Chen, Z. F. Liu, G. C. Guo, J. S. Huang, *Inorg. Chem. Commun.* **2010**, *13*, 250–253.

[6] a) Y. Li, G. Xu, W. Q. Zou, M. S. Wang, F. K. Zheng, M. F. Wu, H. Y. Zeng, G. C. Guo, J. S. Huang, *Inorg. Chem.* **2008**, *47*, 7945–7947; b) F. Chen, F. K. Zheng, G. N. Liu, A. Q. Wu,

M. S. Wang, S. P. Guo, M. F. Wu, Z. F. Liu, G. C. Guo, J. S. Huang, *Inorg. Chem. Commun.* **2010**, *13*, 278–281.
[7] a) W. Ouellette, H. X. Liu, K. Whitenack, C. J. O'Connor, J. Zubieta, *Cryst. Growth Des.* **2009**, *9*, 4258–4261; b) Q. X. Jia, W. W. Sun, C. F. Yao, H. H. Wu, E. Q. Gao, C. M. Liu, *Dalton Trans.* **2009**, 2721–2730.
[8] a) F. Himo, Z. P. Demko, L. Noodleman, K. B. Sharpless, *J. Am. Chem. Soc.* **2003**, *125*, 9983–9987; b) Q. Wang, T. R. Chan, R. Hilgraf, V. V. Fokin, K. B. Sharpless, M. G. Finn, *J. Am. Chem. Soc.* **2003**, *125*, 3192–3193.
[9] F. Chen, F. K. Zheng, G. N. Liu, M. F. Wu, Z. F. Liu, G. C. Guo, *Acta Crystallogr., Sect. E* **2010**, *66*, m758.
[10] J. T. Li, J. Tao, R. B. Huang, L. S. Zhang, *Acta Crystallogr., Sect. E* **2005**, *61*, m984–m985.
[11] a) G. B. Deacon, R. J. Phillips, *Coord. Chem. Rev.* **1980**, *33*, 227–250; b) A. Q. Wu, Y. Li, F. K. Zheng, G. C. Guo, J. S. Huang, *Cryst. Growth Des.* **2006**, *6*, 444–450.
[12] S. S. Tandon, S. D. Bunge, R. Rakosi, Z. Q. Xu, L. K. Thompson, *Dalton Trans.* **2009**, 6536–6551.
[13] a) B. Vangdal, J. Carranza, F. Lloret, M. Julve, J. Sletten, *J. Chem. Soc., Dalton Trans.* **2002**, 566–574; b) Y. S. You, D. Kim, Y. Do, S. J. Oh, C. S. Hong, *Inorg. Chem.* **2004**, *43*, 6899–6901; c) M. S. Wang, G. C. Guo, M. L. Fu, L. Xu, L. Z. Cai, J. S. Huang, *Dalton Trans.* **2005**, 2899–2907.
[14] a) M. A. S. Goher, B. Sodin, B. Bitschnau, E. C. Fuchs, F. A. Mautner, *Polyhedron* **2008**, *27*, 1423–1431; b) Z. Su, J. Xu, Y. Q. Huang, T. Okamura, G. X. Liu, Z. S. Bai, M. S. Chen, S. S. Chen, W. Y. Sun, *J. Solid State Chem.* **2009**, *182*, 1417–1423; c) M. X. Li, H. Wang, S. W. Liang, M. Shao, X. He, Z. X. Wang, S. R. Zhu, *Cryst. Growth Des.* **2009**, *9*, 4626–4633.
[15] Z. Li, M. Li, X. P. Zhou, T. Wu, D. Li, S. W. Ng, *Cryst. Growth Des.* **2007**, *7*, 1992–1998.
[16] a) Q. Y. Liu, L. Xu, *CrystEngComm* **2005**, *7*, 87–89; b) S. K. Ghosh, J. Ribas, M. S. El Fallah, P. K. Bharadwaj, *Inorg. Chem.* **2005**, *44*, 3856–3862.
[17] a) S. Cukierman, *Biophys. J.* **2000**, *78*, 1825–1834; b) K. M. Jude, S. K. Wright, C. Tu, D. N. Silverman, R. E. Viola, D. W. Christianson, *Biochemistry* **2002**, *41*, 2485–2491; c) Y. Schaerli, F. Hollfelder, *Mol. BioSyst.* **2009**, *5*, 1392–1404.
[18] L. E. Cheruzel, M. S. Pometun, M. R. Cecil, M. S. Mashuta, R. J. Wittebort, R. M. Buchanan, *Angew. Chem. Int. Ed.* **2003**, *42*, 5452–5455.
[19] a) R. Cortés, M. Drillon, X. Solans, L. Lezama, T. Rojo, *Inorg. Chem.* **1997**, *36*, 677–683; b) Y. Go, X. Q. Wang, E. V. Anokhina, A. J. Jacobson, *Inorg. Chem.* **2004**, *43*, 5360–5367.
[20] G. H. Tao, B. Twamley, J. M. Shreeve, *Inorg. Chem.* **2009**, *48*, 9918–9923.
[21] Z. P. Yu, Y. Xie, S. J. Wang, G. P. Yong, Z. Y. Wang, *Inorg. Chem. Commun.* **2008**, *11*, 372–376.
[22] a) N. L. Rosi, M. Eddaoudi, J. Kim, M. O'Keeffe, O. M. Yaghi, *Angew. Chem. Int. Ed.* **2002**, *41*, 284–287; b) D. M. Ciurtin, M. D. Smith, H. C. zur Loye, *Chem. Commun.* **2002**, 74–75; c) J. H. Jia, X. Lin, C. Wilson, A. J. Blake, N. R. Champness, P. Hubberstey, G. Walker, E. J. Cussen, M. Schröder, *Chem. Commun.* **2007**, 840–842.
[23] a) V. W. W. Yam, K. K. W. Lo, *Chem. Soc. Rev.* **1999**, *28*, 323–334; b) G. H. Wei, J. Yang, J. F. Ma, Y. Y. Liu, S. L. Li, L. P. Zhang, *Dalton Trans.* **2008**, 3080–3092; c) X. X. Zhao, J. P. Ma, Y. B. Dong, R. Q. Huang, *Cryst. Growth Des.* **2007**, *7*, 1058–1068.
[24] a) L. Fabbrizzi, M. Licchelli, G. Rabaioli, A. Taglietti, *Coord. Chem. Rev.* **2000**, *205*, 85–108; b) T. Hirano, K. Kikuchi, Y. Urano, T. Nagano, *J. Am. Chem. Soc.* **2002**, *124*, 6555–6562; c) H. A. Habib, A. Hoffmann, H. A. Höppe, G. Steinfeld, C. Janiak, *Inorg. Chem.* **2009**, *48*, 2166–2180.
[25] a) R. C. Evans, P. Douglas, C. J. Winscom, *Coord. Chem. Rev.* **2006**, *250*, 2093–2126; b) H. J. Son, W. S. Han, J. Y. Chun, B. K. Kang, S. N. Kwon, J. Ko, S. J. Han, C. Lee, S. J. Kim, S. O. Kang, *Inorg. Chem.* **2008**, *47*, 5666–5676.
[26] S. L. Zheng, X. M. Chen, *Aust. J. Chem.* **2004**, *57*, 703–712.
[27] a) C. Makedonas, C. A. Mitsopoulou, F. J. Lahoz, A. I. Balana, *Inorg. Chem.* **2003**, *42*, 8853–8865; b) I. V. Novozhilova, A. V. Volkov, P. Coppens, *Inorg. Chem.* **2004**, *43*, 2299–2307.
[28] a) A. Rodríguez-Diéguez, A. Salinas-Castillo, S. Galli, N. Masciocchi, J. M. Gutiérrez-Zorrilla, P. Vitoria, E. Colacio, *Dalton Trans.* **2007**, 1821–1828; b) X. L. Tong, D. Z. Wang, T. L. Hu, W. C. Song, Y. Tao, X. H. Bu, *Cryst. Growth Des.* **2009**, *9*, 2280–2286.
[29] M. D. Allendorf, C. A. Bauer, R. K. Bhakta, R. J. T. Houk, *Chem. Soc. Rev.* **2009**, *38*, 1330–1352.
[30] B. Di Bartolo in *Optical Interactions in Solids*, John Wiley & Sons, Inc., New York, **1968**, chapter 18, pp. 432–475.
[31] a) L. A. Riseberg, H. W. Moos, *Phys. Rev.* **1968**, *174*, 429–438; b) M. J. Weber, *Phys. Rev.* **1968**, *171*, 283–291.
[32] a) J. A. Bailey, M. G. Hill, R. E. Marsh, V. M. Miskowski, W. P. Schaefer, H. B. Gray, *Inorg. Chem.* **1995**, *34*, 4591–4599; b) V. H. Houlding, V. M. Miskowski, *Coord. Chem. Rev.* **1991**, *111*, 145–152.
[33] M. Segall, P. Linda, M. Probert, C. Pickard, P. Hasnip, S. Clark, M. Payne, *Materials Studio CASTEP*, version 2.2, Accelrys, San Diego, CA, **2002**.
[34] M. Segall, P. Linda, M. Probert, C. Pickard, P. Hasnip, S. Clark, M. Payne, *J. Phys.: Condens. Matter* **2002**, *14*, 2717–2744.
[35] D. R. Hamann, M. Schluter, C. Chiang, *Phys. Rev. Lett.* **1979**, *43*, 1494–1497.
[36] Siemens, *SHELXTL™ Version 5 Reference Manual*, Siemens Energy & Automation, Inc., Madison, Wisconsin, USA, **1994**.

Received: May 25, 2010
Published Online: September 21, 2010

